International Journal of Mechanical, Industrial and Aerospace Sciences
ISSN: 2517-9950
Vol:11, No:2, 2017

Dynamic Analysis of Offshore 2-HUS/U Parallel Platform

Xie Kefeng, Zhang He

***Abstract*—**For the stability and control demand of offshore small floating platform, a 2-HUS/U parallel mechanism was presented as offshore platform. Inverse kinematics was obtained by institutional constraint equation, and the dynamic model of offshore 2-HUS/U parallel platform was derived based on rigid body's Lagrangian method. The equivalent moment of inertia, damping and driving force/torque variation of offshore 2-HUS/U parallel platform were analyzed. A numerical example shows that, for parallel platform of given motion, system's equivalent inertia changes 1.25 times maximally. During the movement of platform, they change dramatically with the system configuration and have coupling characteristics. The maximum equivalent drive torque is 800 N. At the same time, the curve of platform's driving force/torque is smooth and has good sine features. The control system needs to be adjusted according to kinetic equation during stability and control and it provides a basis for the optimization of control system.

***Keywords*—**2-HUS/U platform, Dynamics, Lagrange, Parallel platform

I. Introduction

THE common offshore floating platforms are mainly oil drilling platforms and wind power equipment platforms [1]-[3]. These resource platforms mostly have the foundation and large size, and work a long time at the same offshore position. Offshore equipment likes unmanned ships and aircraft carrier [4], have advanced control system and communication systems, which can be able to complete sea area task, but their range of motion is limited, and they are still large as targets, which cannot be carried as detection equipment or protection equipment. So, a small portable offshore platform should be designed currently, which can be carried by aircraft of submarine.

The offshore platform will produce attitude deflection of a certain level because of the interference of marine environment (including wave and ocean current). The attitude deflection mainly includes roll and pitch [5]. For the load equipment of the offshore platform, the attitude deflection will have influence on the accuracy and stability of the information collected. Therefore, the offshore platform needs a stabilizing mechanism which can offset or suppress the sea platform deflection caused by wave interference. Common stable platforms include six-axis stable platform [6], [7] and less degrees of freedom (DOFs) stable platform such as three-axis stable platform [8], [9]. They are able to effectively isolate pitching and rolling of the waves. But, the sea floating platform referred here is different from the common stable platform because of limitations of size and sea environment.

According to the requirements of small sea platform, a small offshore 2-HUS/U parallel platform is proposed. This space parallel platform has two DOFs, and is driven by ball screw. In this paper, variations of equivalent inertia, damping and driving forces with time are emphatically investigated.

II. Offshore 2-HUS Parallel Platform Analysis

A. Parallel Platform Structure Description

The structure of offshore 2-HUS/U parallel platform is shown in Fig. 1. Its up-platform PA1A2 and base OC1C2 are all shape disk, and are driven by two driving branched chain and a driven branched chain. The driving branched chain consists of one screw pair (H), one hooke hinge (U), and one ball joint (S), and the driven branched chain consists of one hooke hinge (U). The centers of ball joint (A1, A2) and hooke hinge (P) are located on the up platform, and the points (A1, A2, P) form isosceles right triangle whose Cartesian point is P. The fixed coordinate system O-XYZ is established. The point O is located on the base, and Z axis is vertical upward, and Y axis is located on the angle bisector, and X axis is determined by the right-handed coordinate system. The moving coordinate system P-XYZ is established at the center P of the moving platform, and the initial orientation coincides with the fixed coordinates system.

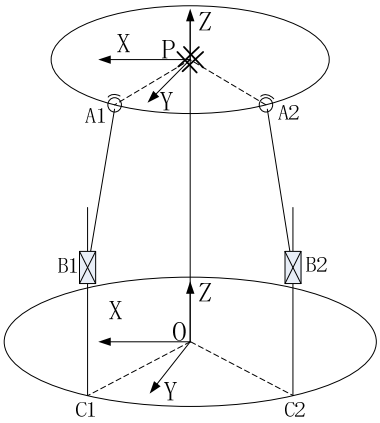

Fig. 1 Sketch diagram of offshore parallel platform

B. Parallel Platform Location Analysis

Offshore 2-HUS/U parallel platform is a space platform and it contains many components. From the amendment of

Xie Kefeng is with Nanjing University of Science and Technology, Nanjing, CO 210094 China (e-mail: xiekefeng.ok@163.com).

Zhang He is with Nanjing University of Science and Technology, Nanjing, CO 210094 China (phone: +86-025-84315694; e-mail: hezhangz@mail.njust.edu.cn).

Grubler-Kutzbach formula [10], it is easily understood that the platform is a two-DOF mechanism. Therefore, the two Euler angles (β,γ) are selected as the generalized coordinates [11].

Suppose that the radius of the moving platform and the base is R, and the length of the link B1C1 and B2C2 is L, and the distance between the point P and O is H. Then, the coordinate of points A1, A2 in moving coordinate system are:

According to the coordinate transformation, the equation is established

$${}^{P}A_1=\left(\frac{\sqrt{2}}{2}\mathrm{R}\quad\frac{\sqrt{2}}{2}\mathrm{R}\quad 0\right)^{\mathrm{T}},\ {}^{P}A_2=\left(-\frac{\sqrt{2}}{2}\mathrm{R}\quad\frac{\sqrt{2}}{2}\mathrm{R}\quad 0\right)^{\mathrm{T}}$$

According to the coordinate transformation, the equation is established

$${}^{O}A_i={}^{O}_{P}\mathbf{T}\,{}^{P}A_i+P \tag{1}$$

where ${}^{O}_{P}T$ is the coordinate transformation matrix, P is the distance between the moving coordinate system and the base, and ${}^{O}A_i$ represents the coordinate of point A_i in base.

$${}^{O}_{P}\mathbf{T}=\begin{bmatrix}\cos\beta & \sin\beta\bullet\sin\gamma & \sin\beta\bullet\cos\gamma\\ 0 & \cos\gamma & -\sin\gamma\\ -\sin\beta & \cos\beta\bullet\sin\gamma & \cos\beta\bullet\cos\gamma\end{bmatrix},P=\begin{bmatrix}0 & 0 & \mathrm{H}\end{bmatrix}$$

Referring to (1), the coordinate of A1 and A2 in base can be obtained.

$${}^{O}A_1=\begin{pmatrix}\frac{\sqrt{2}}{2}R(\cos\beta+\sin\beta\sin\gamma)\\ \frac{\sqrt{2}}{2}R\cos\gamma\\ H-\frac{\sqrt{2}}{2}R(\sin\beta-\cos\beta\sin\gamma)\end{pmatrix} \tag{2}$$

$${}^{O}A_2=\begin{pmatrix}\frac{\sqrt{2}}{2}R(-\cos\beta+\sin\beta\sin\gamma)\\ \frac{\sqrt{2}}{2}R\cos\gamma\\ H+\frac{\sqrt{2}}{2}R(\sin\beta+\cos\beta\sin\gamma)\end{pmatrix} \tag{3}$$

The screw cap of B vertically moves along the screw. Then, the coordinate of points B1, B2 in base coordinate system are:

$${}^{O}B_1=\left(\frac{\sqrt{2}}{2}R\quad\frac{\sqrt{2}}{2}R\quad L_1\right)^{\mathrm{T}},{}^{O}B_2=\left(-\frac{\sqrt{2}}{2}R\quad\frac{\sqrt{2}}{2}R\quad L_2\right)^{\mathrm{T}}$$

The length of the link remains the same in the process of platform moving, and so constraint equation can be obtained:

$$L_i^2=({}^{O}A_i-{}^{O}B_i)^2 \tag{4}$$

Bringing the coordinate of A_i, B_i in base system into (4), it can be obtained:

$$\begin{cases}\mathrm{L}^2=\frac{1}{2}R^2(\cos\beta+\sin\beta\sin\gamma-1)^2+\frac{1}{2}R^2(\cos\gamma-1)^2\\ \quad+(H-\frac{\sqrt{2}}{2}R(\sin\beta-\cos\beta\sin\gamma)-L_1)^2\\ \mathrm{L}^2=\frac{1}{2}R^2(1-\cos\beta+\sin\beta\sin\gamma)^2+\frac{1}{2}R^2(\cos\gamma-1)^2\\ \quad+(H+\frac{\sqrt{2}}{2}R(\sin\beta+\cos\beta\sin\gamma)-L_2)^2\end{cases} \tag{5}$$

By simplifying (5), it can be obtained:

$$\begin{cases}L_1=H-\frac{\sqrt{2}}{2}R(\sin\beta-\cos\beta\sin\gamma)\\ \quad\mp\sqrt{\mathrm{L}^2-\frac{1}{2}R^2(\cos\beta+\sin\beta\sin\gamma-1)^2-\frac{1}{2}R^2(\cos\gamma-1)^2}\\ L_2=H+\frac{\sqrt{2}}{2}R(\sin\beta+\cos\beta\sin\gamma)\\ \quad\mp\sqrt{\mathrm{L}^2-\frac{1}{2}R^2(1-\cos\beta+\sin\beta\sin\gamma)^2-\frac{1}{2}R^2(\cos\gamma-1)^2}\end{cases} \tag{6}$$

By taking a derivative with respect to (6), the movement relationship between the input speed of the link and the generalized coordinates of the moving platform can be obtained.

$$\begin{cases}\dot{L}_1=-\frac{\sqrt{2}}{2}R(c\beta*\dot{\beta}+s\beta s\gamma*\dot{\beta}-c\beta c\gamma*\dot{\gamma})\mp\\ \frac{1}{2}[-R^2(c\beta+s\beta s\gamma-1)(-s\beta*\dot{\beta}+c\beta s\gamma*\dot{\beta}+s\beta c\gamma*\dot{\gamma})\\ -R^2(c\gamma-1)(-s\gamma*\dot{\gamma})]/\sqrt{\mathrm{L}^2-\frac{1}{2}R^2(c\beta+s\beta s\gamma-1)^2-\frac{1}{2}R^2(c\gamma-1)^2}\\ \dot{L}_2=\frac{\sqrt{2}}{2}R(c\beta*\dot{\beta}-s\beta s\gamma*\dot{\beta}+c\beta c\gamma*\dot{\gamma})\mp\\ \frac{1}{2}[-R^2(1-c\beta+s\beta s\gamma)(s\beta*\dot{\beta}+c\beta s\gamma*\dot{\beta}+s\beta c\gamma*\dot{\gamma})\\ -R^2(c\gamma-1)(-s\gamma*\dot{\gamma})]/\sqrt{\mathrm{L}^2-\frac{1}{2}R^2(1-c\beta+s\beta s\gamma)^2-\frac{1}{2}R^2(c\gamma-1)^2}\end{cases} \tag{7}$$

where c represents cos(.), and s represents sin (.).

Equations (3) and (4) are the location and velocity relationship between the driving screw cap and the generalized coordinates of the moving platform.

III. Dynamic Analysis of Offshore Parallel Platform

Analysis of the relationship between generalized coordinates and driving force of offshore parallel platform is related to stress analysis of multi-component. For overcoming the complex features of multi-binding analysis, Lagrangian method [12], [13] is selected. Rigid Lagrange equation is:

$$\frac{\mathrm{d}}{\mathrm{dt}}\frac{\partial L}{\partial\dot{q}_i}-\frac{\partial L}{\partial q_i}=Q_i\ \ (\mathrm{i}=1、2) \tag{8}$$

where L is the Lagrangian function, q_i is the generalized coordinate, Q_i is the generalized force which is acting on the ith generalized coordinate.

Therefore, the relationship between the kinetic or potential energy of each part and the generalized coordinate is mainly analyzed.

A. Analysis of the Kinetic and Potential Energy of up Platform

The movement of up-platform has two DOFs around a fixed point. R is the transformation matrix from the Euler coordinate system to the coordinate system of moving platform. m_s is the quality of moving platform, and I_S is the inertia moments. So, the angular velocity of moving platform in P system is $\omega_S = R \cdot \dot{\varphi}$, and then the kinetic energy of moving platform is

$$T_S = \frac{1}{2}\dot{\varphi}^T \bullet M_S \bullet \dot{\varphi} \tag{9}$$

where

$$M_S = \begin{bmatrix} \mathbf{I}_{sy} \bullet \cos^2\gamma + \mathbf{I}_{sz} \bullet \sin^2\gamma & 0 \\ 0 & \mathbf{I}_{sx} \end{bmatrix},$$

$$\mathbf{I}_S = \begin{bmatrix} I_{sx} & & \\ & I_{sy} & \\ & & I_{sz} \end{bmatrix},\ \mathbf{R} = \begin{bmatrix} 0 & 1 \\ \cos\gamma & 0 \\ -\sin\gamma & 0 \end{bmatrix}$$

The up-platform rotates around the point P. Without considering the friction, its potential energy remains constant, namely $V_S = m_s g \mathrm{H}$.

B. Analysis of the Kinetic and Potential Energy of the Load

The load equipment is fixedly connected with the moving platform, and so its motion state is the same with the moving platform, without higher center of gravity.

m_f is the quality of the load. $\mathbf{I}_f$ is the inertia moments. d_f is the distance between the centroid of the load and the moving platform. Then, the kinetic energy of the load is

$$T_f = \frac{1}{2}\dot{\varphi}^T \bullet M_f \bullet \dot{\varphi} \tag{10}$$

where

$$\mathbf{I}_f = \begin{bmatrix} I_{fx} + m_f d_f^{\,2} & & \\ & I_{fy} + m_f d_f^{\,2} & \\ & & I_{fz} \end{bmatrix},$$

$$\mathbf{M}_f = \begin{bmatrix} (I_{fy} + m_f d_f^{\,2}) \bullet \cos^2\gamma + I_{fz} \bullet \sin^2\gamma & 0 \\ 0 & (I_{fx} + m_f d_f^{\,2}) \end{bmatrix}$$

The height of the centroid is converted to system coordinate system.

$$H_f = d_f \cos\beta \cos\gamma \tag{11}$$

Then the potential energy of the load is

$$V_f = m_f g d_f \cos\beta \cos\gamma \tag{12}$$

C. Analysis of the Kinetic and Potential Energy of Driving Screw

The driving screw is driven by motor and transfers driving force to system. So the screw only has rotational kinetic energy, and potential energy remains constant.

$$T_g = \frac{1}{2} \bullet \dot{\varphi}^T \bullet M_g \bullet \dot{\varphi} \tag{13}$$

where m_g is the quality of the screw, l_g is the inertia moments, H_g is the height of centroid, and ds is the pitch.

$$M_g = \frac{1}{\mathrm{ds}^2} \bullet J^{-1\mathrm{T}} \bullet \begin{bmatrix} \mathrm{l}_g & 0 \\ 0 & \mathrm{l}_g \end{bmatrix} \bullet J^{-1},\ \mathbf{I}_g = \begin{bmatrix} \mathrm{l}_g & 0 \\ 0 & \mathrm{l}_g \end{bmatrix},\ V_g = m_g g \mathrm{H}_g$$

where J^{-1} is the inverse of Jacobian matrix.

D. Analysis of the Kinetic and Potential Energy of Screw Cap

The screw cap moves along the screw vertically, and only has line speed along Z axis. Then, the kinetic energy of screw cap is

$$T_m = \frac{1}{2} \bullet \dot{\varphi}^T \bullet M_m \bullet \dot{\varphi} \tag{14}$$

where m_m is the quality of screw cap.

$$M_m = J^{-1\mathrm{T}} \bullet \begin{bmatrix} \mathrm{m}_m & 0 \\ 0 & \mathrm{m}_m \end{bmatrix} \bullet J^{-1},\ \mathbf{m}_m = \begin{bmatrix} \mathrm{m}_m & 0 \\ 0 & \mathrm{m}_m \end{bmatrix}$$

Then, the potential energy of screw cap is

$$V_m = \mathrm{m}_m g(L1 + L2) \tag{15}$$

where $L1$ ($L2$) is the displacement of screw cap.

E. Analysis of the Kinetic and Potential Energy of Link

On end of the support link is hooke hinge (U), and the other is ball joint (S). The movement law of the link's centroid can be obtained by hooke hinge and ball joint of both ends. The motion state of hooke hinge remains the same with the screw cap, and the motion state of ball joint remains the same with the point Ai on the up platform.

$$V_{Ai} = (\mathbf{P} \bullet \dot{\varphi}) \times \mathbf{R}_{Ai} \tag{16}$$

$$V_{Bi} = \mathbf{J}_B \bullet J^{-1} \bullet \dot{\varphi} \tag{17}$$

and then,

$$V_A = \mathbf{J}_A \bullet \dot{\varphi} \tag{18}$$

$$V_B = \mathbf{J}_B \bullet J^{-1} \bullet \dot{\varphi} \tag{19}$$

where

$$\mathbf{J}_A = \begin{bmatrix} \begin{bmatrix} 0 & 0 & 1 \\ 0 & 0 & 0 \\ -1 & 0 & 0 \end{bmatrix} \bullet R_{A1} & \begin{bmatrix} 0 & \sin\beta & 0 \\ -\sin\beta & 0 & -\cos\beta \\ 0 & \cos\beta & 0 \end{bmatrix} \bullet R_{A1} \\ \begin{bmatrix} 0 & 0 & 1 \\ 0 & 0 & 0 \\ -1 & 0 & 0 \end{bmatrix} \bullet R_{A2} & \begin{bmatrix} 0 & \sin\beta & 0 \\ -\sin\beta & 0 & -\cos\beta \\ 0 & \cos\beta & 0 \end{bmatrix} \bullet R_{A2} \end{bmatrix},$$

$$\mathbf{J}_B = \begin{bmatrix} 0 & 0 & 1 & 0 & 0 & 0 \\ 0 & 0 & 0 & 0 & 0 & 1 \end{bmatrix}^T$$

The line speed of the link's centroid is

$$v_Z = (\mathbf{J}_A + \mathbf{J}_B \bullet J^{-1}) / 2 \bullet \dot{\varphi} \tag{20}$$

Known from the theorem of rotation,

$$(V_A - V_B) = \omega_Z \times \vec{L} \tag{21}$$

Then, the rotational angular velocity is

$$\omega_Z = \mathbf{J}^{-1}{}_{\omega_Z} \bullet (V_A - V_B) \tag{22}$$

where

$$\mathbf{J}_{\omega_Z} = \begin{bmatrix} \begin{bmatrix} 0 & 0 & 0 \\ 0 & 0 & -1 \\ 0 & 1 & 0 \end{bmatrix} \bullet \vec{L} & \begin{bmatrix} 0 & 0 & 1 \\ 0 & 0 & 0 \\ -1 & 0 & 0 \end{bmatrix} \bullet \vec{L} & \begin{bmatrix} 0 & -1 & 0 \\ 1 & 0 & 0 \\ 0 & 0 & 0 \end{bmatrix} \bullet \vec{L} \end{bmatrix}$$

Then, the kinetic energy of link is

$$T_z = \frac{1}{2}\dot{\varphi}^T \bullet \mathbf{M}_{z1} \bullet \dot{\varphi} + \frac{1}{2}\dot{\varphi}^T \bullet \mathbf{M}_{z2} \bullet \dot{\varphi} \tag{23}$$

where m_{Zi} (i=1、2) is the quality of the support link, I_{Zi} (i=x、y、z) is the principal inertia moments of the support link.

$$m_{z1} = (\mathbf{J}_A + \mathbf{J}_B \bullet J^{-1})^T m_Z (\mathbf{J}_A + \mathbf{J}_B \bullet J^{-1}) / 4,$$

$$m_{z2} = (\mathbf{J}_A - \mathbf{J}_B \bullet J^{-1})^T \bullet J^{-1T}{}_{\omega_Z} I_Z J^{-1}{}_{\omega_Z} \bullet (\mathbf{J}_A - \mathbf{J}_B \bullet J^{-1}),$$

$$m_Z = diag(\mathrm{m}_{z1} \quad \mathrm{m}_{z1} \quad \mathrm{m}_{Z1} \quad \mathrm{m}_{z2} \quad \mathrm{m}_{z2} \quad \mathrm{m}_{z2}),$$

$$I_Z = diag(\mathrm{I}_{Zx} \quad \mathrm{I}_{Zy} \quad \mathrm{I}_{Zz})$$

The height of the link's centroid along Z axis is

$$h_z = (L1 + L2 + {}^0A_1(3) + {}^0A_2(3)) / 2 \tag{24}$$

Then, the potential energy of the link is

$$V_z = m_z g (L1 + L2 + {}^0A_1(3) + {}^0A_2(3)) / 2 \tag{25}$$

F. Lagrange Dynamic Equation

Lagrangian function can be determined from (9)-(25).

$$L(\varphi, \dot{\varphi}) = \frac{1}{2}\dot{\varphi}^T \bullet M(\varphi) \bullet \dot{\varphi} + V(\varphi) \tag{26}$$

where

$$M(\varphi) = M_S + M_f + M_g + M_m + M_{z1} + M_{z2},$$

$$V(\varphi) = m_s g H + m_f g h_f \cos\beta \cos\gamma + m_g g H_g + m_m g (L1 + L2) + m_z g (L1 + L2 + {}^0A_1(3) + {}^0A_2(3)) / 2.$$

Bringing (26) into (8), dynamic equation can be obtained.

$$M(\varphi)\ddot{\varphi} + C(\varphi, \dot{\varphi})\dot{\varphi} + N(\varphi, \dot{\varphi}) = \tau \tag{27}$$

where $M(\varphi)$ is the inertia matrix of the system. $C(\varphi, \dot{\varphi})$ is the Coriolis matrix of the system, which contains Coriolis forces and centrifugal forces during movement. $N(\varphi, \dot{\varphi})$ is the potential force of the system. If friction is present in system, $N(\varphi, \dot{\varphi})$ also contains conservative force generated by friction.

The Coriolis matrix [14] can be obtained by the inertia matrix.

$$C_{ij}(\varphi, \dot{\varphi}) = \sum_{k=1}^{n} \Gamma_{ijk} \dot{\varphi}_k = \frac{1}{2} \sum_{k=1}^{n} \left\{ \frac{\partial M_{ij}}{\partial \varphi_k} + \frac{\partial M_{ik}}{\partial \varphi_j} - \frac{\partial M_{kj}}{\partial \varphi_i} \right\} \dot{\varphi}_k \tag{28}$$

The inertia matrix is written as

$$M(\varphi) = \begin{bmatrix} M_{11} & M_{12} \\ M_{21} & M_{22} \end{bmatrix} \tag{29}$$

$$C_{11}(\varphi, \dot{\varphi}) = \frac{1}{2}(A\dot{\beta} + D\dot{\gamma}) \tag{30}$$

$$C_{12}(\varphi, \dot{\varphi}) = \frac{1}{2}(D\dot{\beta} + 2E\dot{\gamma} - C\dot{\gamma}) \tag{31}$$

$$C_{21}(\varphi, \dot{\varphi}) = \frac{1}{2}(2 \bullet B\dot{\beta} - D\dot{\beta} + C\dot{\gamma}) \tag{32}$$

$$C_{22}(\varphi, \dot{\varphi}) = \frac{1}{2}(C\dot{\beta} + F\dot{\gamma}) \tag{33}$$

where

$$A=\frac{\partial M_{11}}{\partial \beta},\ B=\frac{\partial M_{21}}{\partial \beta},\ C=\frac{\partial M_{22}}{\partial \beta},\ D=\frac{\partial M_{11}}{\partial \gamma},\ E=\frac{\partial M_{12}}{\partial \gamma},$$

$$F=\frac{\partial M_{22}}{\partial \gamma}.$$

$$N_1(\varphi,\dot{\varphi})=\frac{\partial V}{\partial \beta} \tag{34}$$

$$N_2(\varphi,\dot{\varphi})=\frac{\partial V}{\partial \gamma} \tag{35}$$

In (27), τ is the generalized force corresponding to the generalized coordinate. $M(\varphi)$ is the equivalent inertia of system and it is related to the shape and size of the platform, thus it is affecting the dynamic characteristics of the offshore parallel platform.

IV. Example Analysis of Offshore Parallel Platform

The materials of each part are steel, and the material density is 7800 kg/m^3. The length of the link is 300 mm. The pitch of the screw is 1. The rest parameters of the system are shown in Table I. It is assumed that the moving platform rotates continuously, and its movement is

$$\begin{cases}\beta(t)=\dfrac{\pi}{4}\sin(\omega t+t_0)\\ \gamma(t)=\dfrac{\pi}{4}\sin(\omega t)\end{cases} \tag{36}$$

TABLE I
Parameters of Each Part

Part	Quantity (kg)	Ixx (kg*m^2)	Iyy (kg*m^2)	Izz (kg*m^2)
Up platform	30	0.47	0.47	0.95
Screw	4.3	×	×	0.00076
Screw cap	7.5	×	×	0.02
Link	10	0.04	0.04	0.05
Load	140	20	20	25

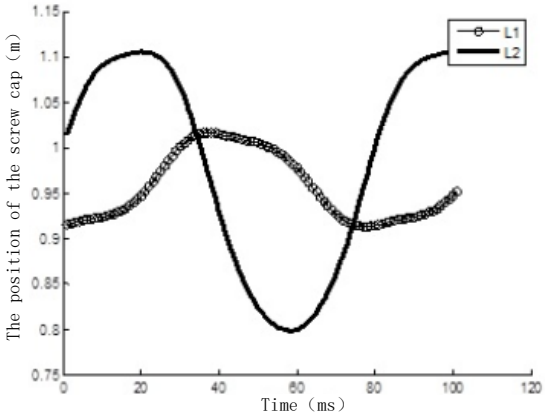

Fig. 2 The position curve of the driving screw cap

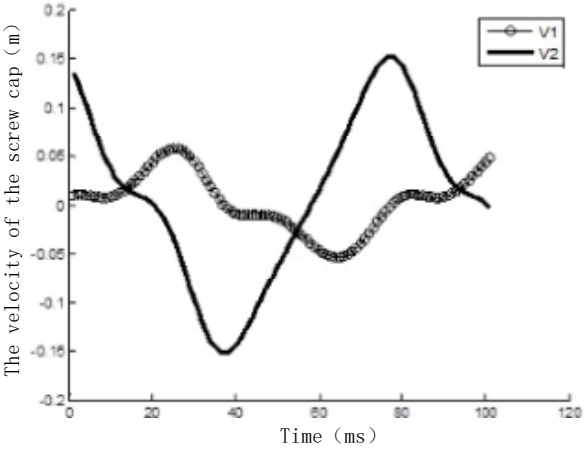

Fig. 3 Velocity curve of the driving screw cap

For the given movement of the up-platform, the movement of the link can be obtained by the inverse kinematics. Figs. 2 and 3 are the position and velocity curve of the driving screw cap on the up platform, respectively. From these figures, it can be seen that the movement of two caps is in line with the sine law, but the position of the cap 2 near the apex will generate a certain degree of distortion, as the same with the velocity of the cap 2. The reason is that the movement of the nut 2 is coupled with two DOFs.

For the given movement, the curves of M_{11}, M_{12}, M_{21}, M_{22} are shown in Fig. 4. Obviously, these equivalent inertias are the function of the size and shape of the system, and their values are constantly changing as the movement of system. Compared to the M_{11}, the equivalent inertia M_{22} changes dramatically, and the maximum change is 1.25 times. But the change characteristic of the primary inertia remains the same with the movement of the system. In Fig. 4 (b), for the equivalent inertia matrix is symmetric matrix, the equivalent inertia M_{12} completely coincides with M_{21}. Compared to the primary inertia, their variation produces a certain distortion at the extremes on the basis of the sine curve. The change characteristics of the equivalent inertia also determine the dynamic motion characteristics of the system. As shown in Fig. 5, damping curves keep good sinusoidal characteristic.

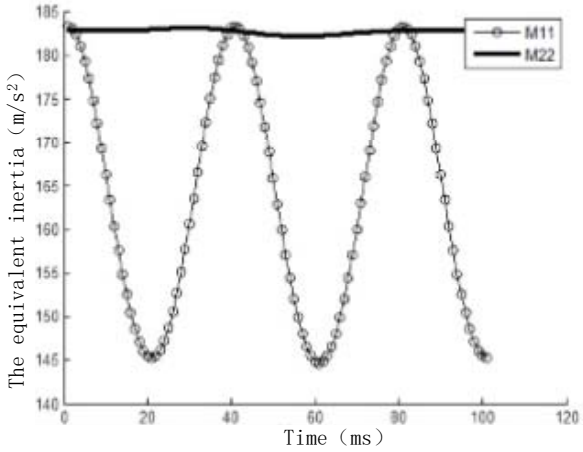

(a)

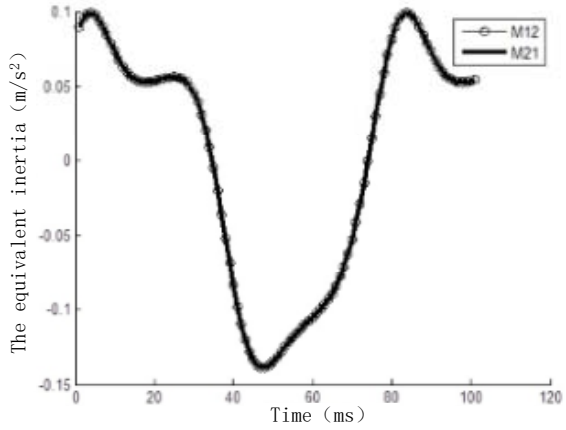

(b)

Fig. 4 Equivalent inertia curve of parallel platform

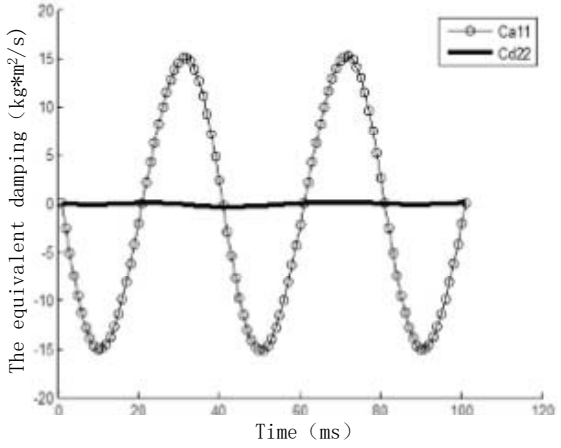

(a)

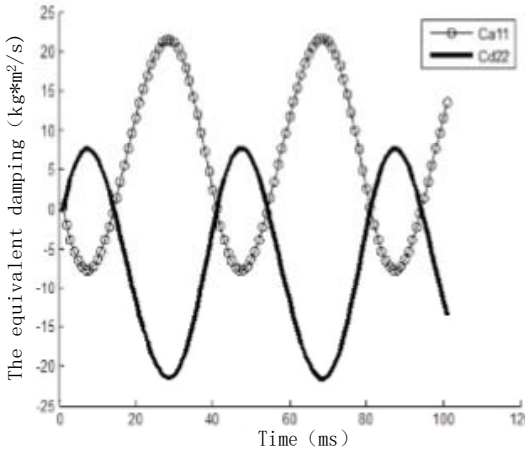

(b)

Fig. 5 Damping curve of parallel platform

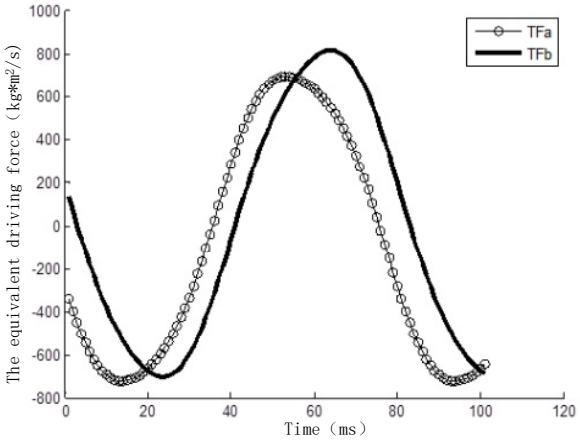

(a)

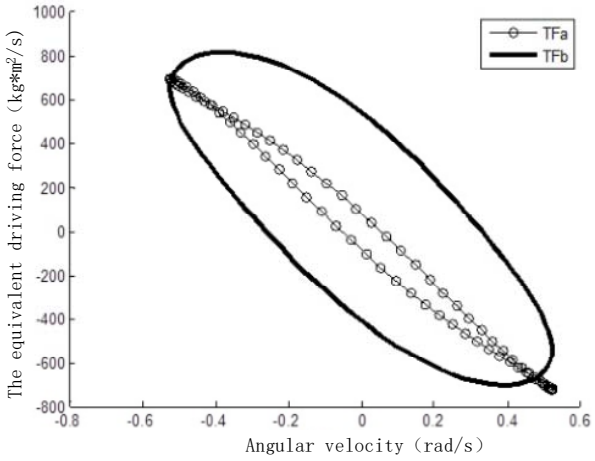

(b)

Fig. 6 Equivalent driving force curve of parallel platform

For the given movement of the up platform, the variation curves of two generalized driving force (torque) of the screw

cap are shown in Fig. 6. Fig. 6 (a) is the variation curve of the driving force over time, and Fig. 6 (b) is the variation curve of the driving force over angular velocity. During the movement of the parallel platform, the driving force changes within 800 N. It is easier to select the driving motor for the little range. The phase difference of the variation curve is 30°, and the curves have good sine law, forming a central symmetry, which prove the correctness of derivation of kinetic equations and the reasonableness of system architecture design. As can be seen from the above analysis, within 30° variation width, for the load of 140kg, the maximum driving speed of the system is less than 100m/s, and the maximum driving force is less than 800N, which meet the needs of three sea conditions.

V. Conclusion

A small offshore 2-HUS/U parallel platform structure is presented. For the two degrees of freedom hooke hinge, the structural characteristics were analyzed, and the inverse kinematics and velocity solution of the driving screw cap are obtained. Using Lagrangian method, a dynamic model of the offshore 2-HUS/U parallel platform is created, and then the variation of the equivalent inertia and equivalent driving force of the system are analyzed. Through the examples, the position and velocity curves of driving screw cap are given, and the variation curve of the equivalent inertia and generalized driving force (torque) are given. The variation curve describes the correctness of derivation of kinetic equations and the reasonableness of system architecture design, and at the same time, through a drastic change of the equivalent inertia shows the strong relationship between the equivalent inertia and the shape or size of the mechanism. Therefore, when selecting the driving source and control system parameters, it should adapt to the variation of the equivalent inertia and driving force. Through the whole analysis of the system, the new platform can meet the steady demand for offshore swing amplitude 30°.

References

[1] Z. Y. Wang, B. Zhang, and G. H. Liu, "Application and Foreground of the Floating Structures," *China Offshore Platform*, vol. 24, no. 1, pp.10-14, Feb. 2009.
[2] H. J. Deng. *Study on stability and Mooring System Performance of Offshore Floating Turbine Foundation*. Harbin: Harbin Engineering University, 2012, pp. 2-4.
[3] Q. J. Lu, Z. H. Yang, "Probabilistic dynamic optimization design for support structure of offshore wind turbines," *Journal of vibration and shock*, vol. 32, no. 17, pp.46-51, July, 2013.
[4] Z. W. Hu, H. Chen, J. P. Liu, ''Talang Elf-unmanned surface warship," *Modern Military*, vol. 29, no. 12, pp.44-46, Dec. 2004.
[5] T. H. Ren. *Design and Research of Servo System of Shipboard Stabilized Platform*. Xia men: Xia men University, 2014, pp. 6-7.
[6] X. Liu, T. S. Zhao, and J. W. Gao, "Dynamic Modeling and Analysis of Ship-based Stabilizing Platform in Non-inertial System," *ROBOT*, vol. 36, no. 4, pp.411-418, July, 2014.
[7] X. Y. Sun, Z. J. Xie, K. L. Zhai, and J. Zhang, "Dynamic Analysis and Simulation of 6-PSS Flexible Parallel Robot," *Transactions of the Chinese Society for Agricultural Machinery*, vol. 43, no. 7, pp. 194-205, July, 2012.
[8] H. W. Luo, J. Zhang, H. Wang, and T. Huang, "An Elastodynamic Modeling Method for a 3-RPS Parallel Kinematic Machine," *ROBOT*, vol. 36, no. 6, pp. 737-743, 750. Nov. 2014.
[9] S. Z. Liu, Y. Q. Yu, Q. B. Liu, L. Y. Su, and G. N. Si, "Dynamic Analysis of 3-RRC Parallel Manipulator,". *Journal of Mechanical Engineering*, vol. 45, no. 5, pp. 220-224, May, 2014.
[10] Z. Huang, Y. S. Zhao, T. S. Zhao, *Advanced Spatial Mechanism*. Beijing: Higher Education Press,2006, ch. 5.
[11] K. X. Li, H. Zhang, "Motion Simulation of Stabilized Platform with Parallel Mechanism," *Computer Simulation*, vol. 30, no. 8, pp.212-215, Aug. 2013.
[12] J. W. Zhao, X. G. Ruan, "Modeling and Control of a Flexible Two-wheel Upright Self-balance Humanoid Robot," *ROBOT*, vol. 31, no. 2, pp.179-186, Mar. 2009.
[13] X. Wang, X. G. Yuan, X. Yang, "Research on Multi-Body Separation Dynamics Using Lagrange Method," *Journal of Northwestern Polytechnical University*, vol. 32, no. 1, pp.18-22, Feb. 2014.
[14] M. Richard, Z. X. Li, and S. Charnka, *A Mathematical Introduction to Robotic Manipulation*. Beijing: China Machine Press,1997, ch. 4.